

## Importance of O<sub>2</sub> measurements during photoelectrochemical water-splitting reactions

In pursuit of clean and renewable energy sources, harvesting solar energy has been recognized as the most sustainable route.<sup>1-4</sup> However, the diffuse and intermittent nature of the solar energy reduces the overall dependency and utilization.<sup>5,6</sup> A potential solution for maximum utilization of solar energy is to directly convert it into storable fuels in terms of chemical bonds (such as hydrogen from water).<sup>6-8</sup> In this context, solar-driven photoelectrochemical (PEC) water splitting is a promising approach that can potentially commercialize hydrogen production from renewables.<sup>9, 10</sup> Since the demonstration of PEC water oxidation on an n-type rutile TiO<sub>2</sub> single-crystal electrode by Honda–Fujishima in the early 1970s,<sup>11</sup> PEC water splitting on various semiconducting materials has been studied.<sup>10, 12, 13</sup> A large fraction of technologically important semiconductors (such as Si, and other III-Vs) are not capable of driving unassisted (without bias) water splitting due to their limited photovoltage produced by light illumination. Hence, it is important to utilize series connected or tandem light absorbing devices, to achieve the required potential (~1.7-1.8V). In this context, tandem PEC devices based on a-Si and III-V based semiconductors have been used for water splitting,<sup>14, 15</sup> and overall solar to hydrogen efficiencies (STH) > 10% has been reported.<sup>16-20</sup>

However, the instability of these PEC devices prohibit their practical use for solar-driven water splitting. Almost all non-oxide semiconductors such as Si, Ge, GaAs, InGaN, GaP etc. suffer from photocorrosion under the reaction conditions (highly acidic/basic electrolytes at a potential > 1.8 V). Various protection strategies such as the deposition of thin metal and metal oxide films have been implemented, which has enhanced stability to a few hours.<sup>16, 20-26</sup> Yet most of the PEC stability testing has been performed primarily by monitoring the photocurrent density or the amount of H<sub>2</sub> produced, and not much importance has been given to O<sub>2</sub> measurements.<sup>20, 27-32</sup> Complications in measuring the

omnipresent  $O_2$  during the reaction is understandable but relying only on current density and hydrogen production rate may be erroneous especially due to the probable oxidation of the semiconductor rather than water.

In this work, we provide evidence on the importance of oxygen measurements during PEC water splitting experiments and demonstrate how the current density and hydrogen measurements may distort and leads to erroneous stability data over time. To prove the concept, we performed a series of PEC water splitting experiments by employing triple junction (3J) InGaP/InGaAs/Ge photoelectrochemical (PEC) cell in a photoanode configuration with and without the surface protection. Here we employed atomic layer deposited (ALD)- $TiO_2$  thin films, the most commonly used material and technique for the purpose of surface protection. The PEC experiments with and without the surface protection layer demonstrate that the 3J photoanode corrodes over time, demonstrating that the 3J photoanode does not oxidize the water but as a sacrificial inorganic compound, the photoanode is corroded through self-oxidation. This is evident only through  $O_2$  measurements as we discovered how photocurrent or  $H_2$  measurements could be misleading. Finally, for demonstration purposes we also employed a thin-foil of Ti (0.25 mm thickness) as a surface protection layer for the 3J photoelectrode that showed true water-splitting activity as evidenced by stoichiometric ratio (2:1) of hydrogen and oxygen gases. Overall, we believe that our finding will encourage researchers working in the field of PEC to conduct the additionally desired step of measuring both the  $H_2$  and  $O_2$  gases and quantify them to demonstrate the stability and set a standard method for evaluating the PEC activity.

Figure 1(a) presents the 3J PEC device employed in a photoanode configuration in which the front side was for light absorption purpose and backside for PEC water-oxidation reaction. Before measuring the PEC performance, photovoltaic (PV) characteristics of the InGaP/InGaAs/Ge solar cell was measured under AM 1.5G illumination and the results are shown in Figure 1(b). Under simulated sunlight, the current density ( $J_{sc}$ ), the open-circuit voltage ( $V_{oc}$ ) and the fill factor (FF) were  $13.5 \text{ mAcm}^{-2}$

<sup>2</sup>, 2.54 V and 0.82, respectively. Three types of experiments were as follows: (a) the first one is using the 3J photoanode without surface protection layer; (b) the second is using protection layer made of ~40 nm thick TiO<sub>2</sub>, deposited by atomic layer deposition (ALD); (c) the third one is upon using a protection layer made of a Ti-foil (250 μm). All the samples had 5 nm thick Pt sputtered as OER catalyst.

**A. PEC water splitting without surface protection layer:** The PEC testing of InGaP/InGaAs/Ge photoanode was carried out using cyclic voltammetry (CV) in a gas-tight quartz cell without any uncompensated resistance (iR) correction. Three-electrode measurement setup consists of a Pt counter electrode, a standard Ag/AgCl electrode, and a PEC cell as working electrode in 1.0 M Na<sub>2</sub>SO<sub>4</sub> (pH ~ 7) (aq.) electrolyte under one sun AM 1.5G illumination. During measurements, the light harvesting side is illuminated through a thin quartz substrate (0.5 mm thick), while the Pt catalyst on the back side of the PEC device is in contact with the electrolyte to drive the OER. The results show that (Figure 2a) the CV performance matches closely the PV performance, with a  $J_{sc}$ , and  $V_{oc}$ , of 9.5 mA cm<sup>-2</sup>, and 2.2 V, respectively, and with a power conversion efficiency of 12.4%. The  $V_{oc}$  of 2.2 V for the PEC cell is ~0.2 V less than the  $V_{oc}$  measured in air, which is mainly attributed to kinetic overpotential losses.<sup>33</sup> The PEC stability was initially evaluated by a continuous chronoamperometry under one sun illumination in the neutral (1.0 M Na<sub>2</sub>SO<sub>4</sub>) electrolyte at 0.61 V vs RHE. Stability results indicate that the photocurrent is stable for over 10 h of operation with almost no sign of decay (Figure 2(b)). Besides, H<sub>2</sub> gas produced during the reaction was measured using an online gas chromatogram. The H<sub>2</sub> production rate is consistent with the photocurrent trend and found to be stable as a function of reaction time [Figure 1(b)]. Most of the articles published on PEC water splitting consistently report the photocurrent or H<sub>2</sub> production-based results without accounting the O<sub>2</sub> production. We further measured the O<sub>2</sub> production during the PEC water splitting reaction to confirm whether the reaction has occurred through true water splitting mechanism with proper H<sub>2</sub>/O<sub>2</sub> ratio of 2:1. Figure 1(c) shows the O<sub>2</sub>

production and  $\text{H}_2/\text{O}_2$  ratio obtained during the PEC reaction using Pt coated 3J photoanode. Unexpectedly,  $\text{O}_2$  production significantly drops within 30 min of reaction and no further  $\text{O}_2$  is detected. Thus, the  $\text{H}_2/\text{O}_2$  ratio is quite deviated from the expected 2:1 ratio for water splitting. Therefore, only relying on photocurrent and  $\text{H}_2$  production measurements without considering  $\text{O}_2$  production can be misleading. Furthermore, this problem is accentuated when the experiment was conducted in a two-electrode setup without any applied bias (Supporting information: Figure S1). As shown in Figure S1, the calculated STH efficiency based on photocurrent is  $\sim 9.84\%$  and  $\sim 9.24\%$  based on  $\text{H}_2$ . Overall, the device is stable for more than 6 hours without any obvious degradation in current density or  $\text{H}_2$  evolved. However, since no  $\text{O}_2$  was produced during the reaction, the STH efficiency numbers do not have any meaning. Here it is also important to point out that accurate efficiency determination for water splitting becomes difficult when operated with a bias (in a three electrode setup) and under half-cell conditions since the counter electrode is not maintained at a constant bias.

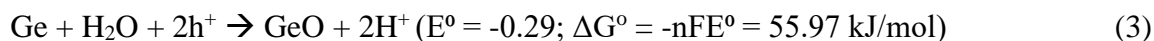
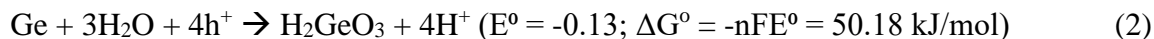
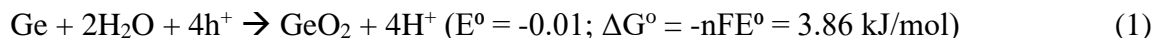
**B. PEC water splitting with ALD-TiO<sub>2</sub> protection:** Amorphous TiO<sub>2</sub> thin films deposited by ALD have been widely used to protect III-V based PEC cells with reported stability up to 100 hours.<sup>19, 20</sup> These thin TiO<sub>2</sub> films are termed “leaky oxide” referring to increase in conductivity due to the amorphous nature.<sup>34-36</sup> In this context, we have carried out PEC stability testing of ALD-TiO<sub>2</sub> protected 3J cell. The ALD-TiO<sub>2</sub> films were deposited at 150 °C for 1000 cycles using titanium tetraisopropyl oxide (TIIP) as a precursor and H<sub>2</sub>O as the reactant. The dosing time was kept at 1 second per pulse for TIIP and 0.1 second per pulse for H<sub>2</sub>O. The thickness of TiO<sub>2</sub> layer was  $\sim 40$  nm as determined by electron microscopy (Supporting information: Figure S2 and S3). This was followed by preparing a 5 nm thick layer of Pt (by sputtering) on top of TiO<sub>2</sub> as an OER catalyst. Figure 3(a) shows the CV curve of the ALD-TiO<sub>2</sub> protected 3J photoanode in 1.0 M Na<sub>2</sub>SO<sub>4</sub> (pH  $\sim 7$ ) under 1-sun AM 1.5G illumination. At 0 V vs RHE we observed  $\sim 7.7$  mA/cm<sup>2</sup> and the photocurrent saturates to  $\sim 9.4$  mA/cm<sup>2</sup> at 0.2 V vs RHE. The PEC

stability testing was carried out under identical conditions as the previous test and a stable photocurrent and hydrogen production were observed up to 8 h as shown in Figure 3(b). However, as shown in Figure 3(c), the stable oxygen production was observed during the initial ~1.5 h with H<sub>2</sub>/O<sub>2</sub> ratio of 2:1. The oxygen production rates, afterward, have abruptly dropped to zero after 2 h of continuous reaction. Yet, as noticed above the current density and the hydrogen production rate do not show evidence of instability. Hence, O<sub>2</sub> gas should be measured throughout the total duration of the experiment and not at a selected timeframe.

The results of experiments (A) and (B) indicate that upon contact with the electrolyte the 3J photoanode does not oxidize water but acts as a sacrificial compound. Instead of water photo-oxidation, the preferred reaction could be the Ge photo-oxidation; similar to the use of sacrificial agents in powder based photocatalysts.<sup>37-39</sup> Till date powder photocatalysts demonstrate very low solar energy conversion,<sup>39-41</sup> which led to the use of sacrificial agents as electron donors (hole traps) for hydrogen production.<sup>42, 43</sup> The presence of sacrificial donors drove researchers to probe the reductive/oxidative cycles selectively and understand the electron-transfer mechanism.<sup>39-43</sup> However, the use of sacrificial agents does not represent true water-splitting as the oxidative process involves oxidation of the sacrificial agent (forming CO<sub>2</sub>) rather than oxidizing the water to form O<sub>2</sub>.<sup>43</sup> In principle, water-splitting reaction should yield H<sub>2</sub> and O<sub>2</sub> in the stoichiometric ratio of 2:1, which is simply not in the case of employing any form of sacrificial agents.<sup>39-43</sup> Such discrepancies has been recently highlighted,<sup>43</sup> where the authors observed the performance of the photocatalysts in presence of electron donors are not comparable and hence the knowledge acquired by employing such electron donors may not be transferrable.

In this particular case, Ge was used as a sacrificial compound, which eventually destroyed the photoelectrode. The photo-oxidation of the Ge layer during PEC reaction is illustrated in Scheme 1. Photogenerated holes (h<sup>+</sup>) oxidize the semiconductor first, rather than water molecules. This is dependent on the position of  $\phi_{\text{Ge}}^{\text{ox}}$  (oxidation potential) relative to  $\phi_{\text{H}_2\text{O}}(\text{O}_2/\text{H}_2\text{O})$ , and  $\phi_{\text{Ge}}^{\text{re}}$  (reduction)

relative to  $\phi_{\text{H}_2\text{O}}(\text{H}^+/\text{H}_2)$ . For Ge the oxidation potential is  $\sim -0.1$  V vs NHE. Thus, photo-generated holes would rather oxidize Ge than water. In this case, the reaction may proceed as given in (1) – (3):



In the case of semiconductors like Si, its oxidation leads to the formation of metal oxide ( $\text{SiO}_2$ ) on the surface which may act as a passivation layer.<sup>44</sup> But in the case of Germanium, the amorphous  $\text{GeO}_x$  formed on surface is known to be water soluble thus causing the entire layer to slowly disintegrate/etch away during reaction.<sup>45, 46</sup> We have observed that these unprotected III-V cells disintegrate during the PEC reaction and starts breaking into small pieces.

To further analyze the corrosion process the III-V cells were studied by scanning transmission electron microscope (STEM). Figure 4(a) and (b) show cross sectional STEM high-angle annular dark-field imaging (HAADF) images of the 3J (InGaP/InGaAs/Ge/Au) cell after  $\sim 12$  hours of PEC reaction of Figure 2(b). We observe a thick irregular amorphous layer forms on the bottom surface of the 3J cell. Elemental mapping using energy filtering in Figure 4(c) gives a clearer picture of the extent of corrosion. The elemental mapping indicates that the thick amorphous structure (marked as # 1) is a mixture of a mix of  $\text{GeO}_x/\text{GaO}_x$  as indicated by presence of oxygen, gallium, and small concentration of germanium and arsenic. Thus, the photocorrosion and mechanical disintegration of the 3J cell leads to loss of bottom subcells InGaAs and Ge respectively. The 2<sup>nd</sup> layer observed looks to be the top subcell of InGaP as indicated by the strong concentration of indium and phosphorous. Finally, the third layer (layer # 3) looks like the capping layer, which is GaAs as indicated by presence of gallium and arsenic. Similar corrosion was also observed in cells protected with amorphous  $\text{TiO}_2$  thin films (Supporting information: Figure S4).

**C. PEC water splitting with Ti-thin foil protection:** Finally, we have protected the 3J photoanode using a thin-Ti foil (0.25 mm thick, 99% purity, ALFA AESAR) on which Pt was deposited in a similar manner. Ti is a widely studied protection layer for various photoelectrodes in different pH conditions.<sup>47</sup> It forms a native oxide passivation layer ~2-4 nm thick, which further protects the PEC cell from corrosion.<sup>48, 49</sup> Figure 5(a) shows the CV of the Ti foil protected 3J photoanode in 1.0 M Na<sub>2</sub>SO<sub>4</sub> (pH ~ 7) under similar experimental conditions to the previous experiments. Pt/Ti/3J photoanode exhibits a maximum current density ~ 4.6 mA/cm<sup>2</sup> at 0V vs RHE and the light limiting photocurrent saturates to ~ 8.5 mA/cm<sup>2</sup> at 0.35 V vs RHE. As shown in Figure 5(b), Pt/Ti/3J photoanode displays stable photocurrents and hydrogen measurements up to 24 h of continuous reaction time. More importantly, the oxygen production was stable during the entire reaction as shown in Figure 5(c). The H<sub>2</sub>/O<sub>2</sub> ratio was 2:1, indicating the “true” water splitting reaction on Ti-foil protected 3J photoanode. From these results, it is clear that measurement of oxygen is vital to evaluate the stability of PEC photoelectrodes/devices.

Most PEC water splitting studies report photocurrents or hydrogen gas measurements. These can be largely misleading, since the complete catalytic cycle is not monitored, nor given. It is important to measure molecular oxygen when working with unstable semiconductors such as Si, Ge, GaAs, and nitride or sulfide semiconductors for light driven water splitting applications. A catalytic reaction by definition means that a reactive site has contributed into the reaction without itself being destroyed. In that regard a turn over number (which is the integration of total amount of molecular hydrogen divided by the total number of atoms (not only on the surface) of the catalytic material used) needs to be given if measurements of molecular oxygen were found to be difficult. Researchers, referees, and editors investigating and evaluating the water-splitting reaction would benefit from a standard methodology for activity measurements. It is clear based on the above experiments that while photocurrent or H<sub>2</sub>

measurements can be used for initial screening, they cannot be relied on to evaluate stability, calculate reaction rates, or provide a solar to hydrogen efficiency number.



**Figures:**

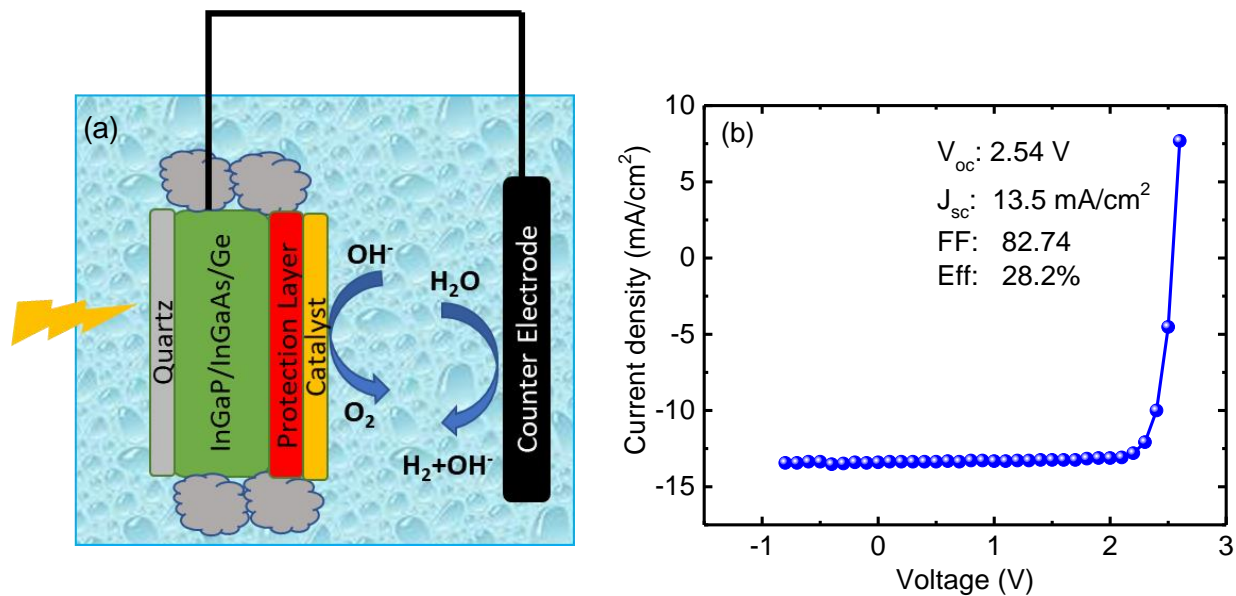


Figure 1. a) Schematic architecture of PEC device made using the InGaP/InGaAs/Ge 3J PV cell. b) J-V characteristics of the InGaP/InGaAs/Ge 3J PV cell measured in air under 1 sun AM1.5G illumination.

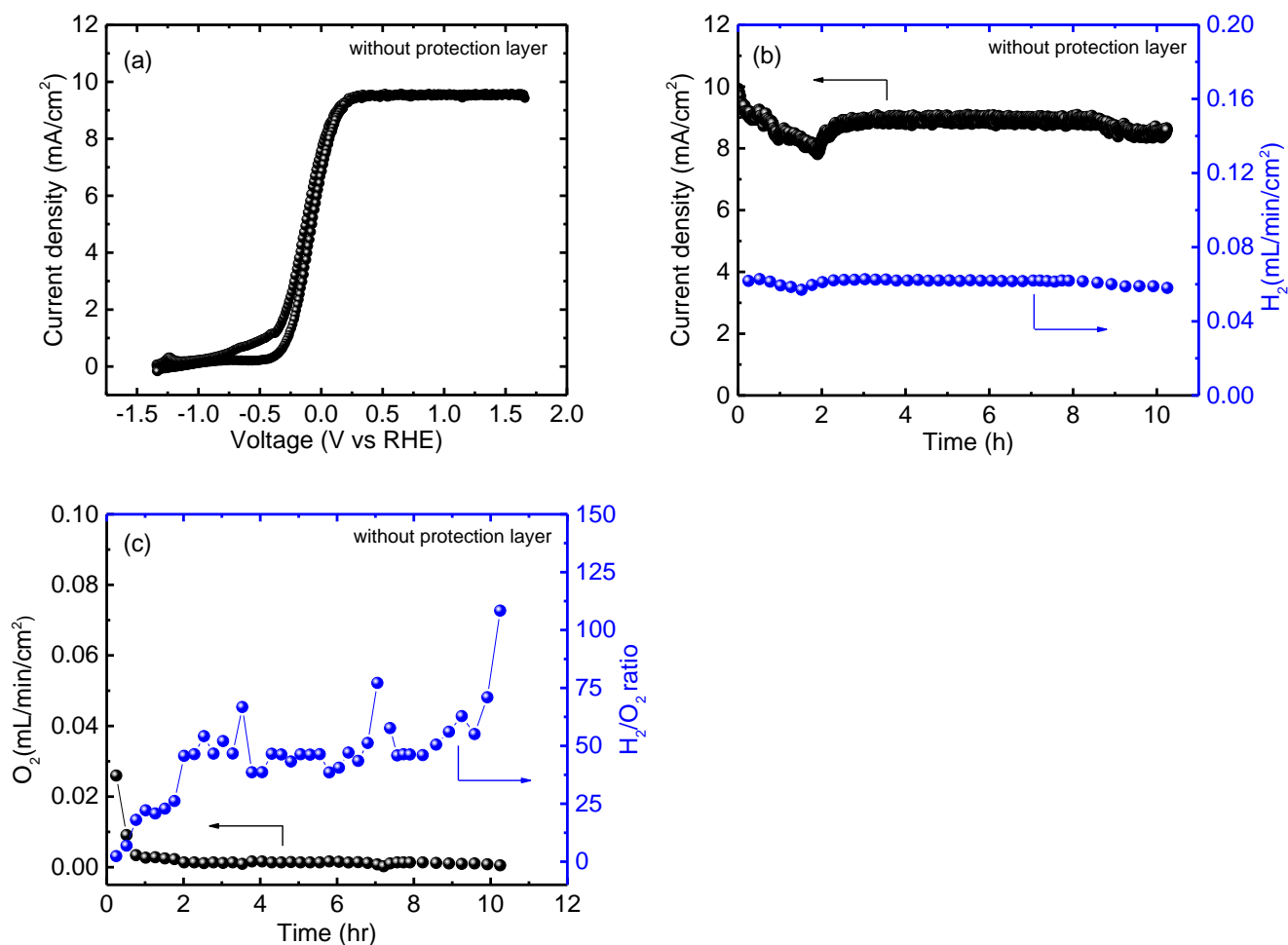


Figure 2. a) Cyclic voltammety (CV) of a 5nm layer thick Pt-coated 3J photoanode measured under three-electrode system in 1.0 M  $\text{Na}_2\text{SO}_4$  (pH  $\sim$  7) under 1 AM 1.5G illumination. b) Chronoamperometry test of a) under AM 1.5G in 1.0 M  $\text{Na}_2\text{SO}_4$  (pH  $\sim$  7) at 0.61 V vs RHE. Left axis shows photocurrent density while right axis shows  $\text{H}_2$  volumetric rates during the reaction. c) The left axis shows volumetric  $\text{O}_2$  rates during chronoamperometry experiment of (b), the right axis displays the calculated  $\text{H}_2$ :  $\text{O}_2$  ratios.

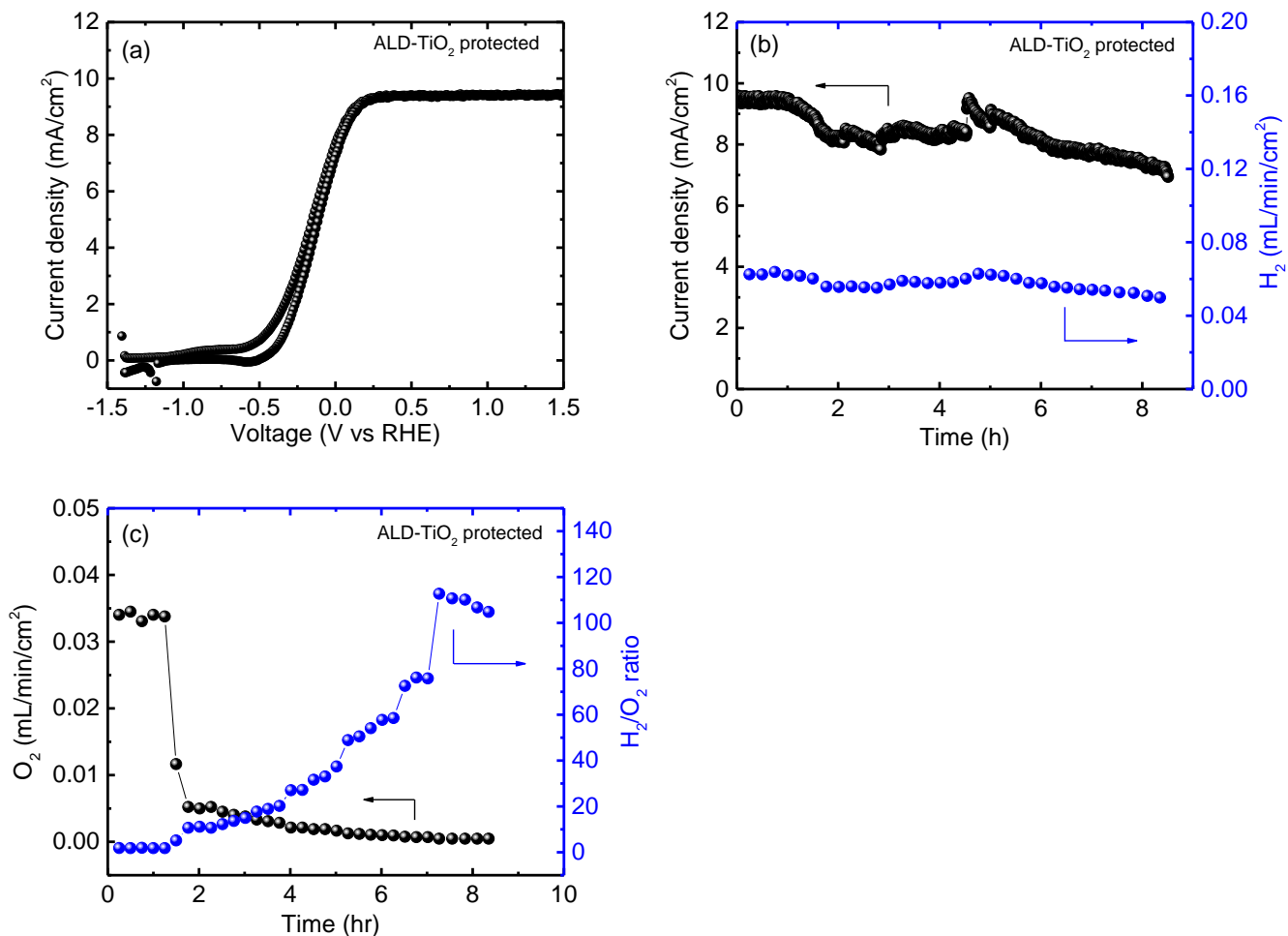


Figure 3. a) Cyclic voltammetry (CV) of the ALD TiO<sub>2</sub> protected 5nm layer thick Pt/Pt<sub>3</sub>J photoanode measured under three-electrode system in 1.0 M Na<sub>2</sub>SO<sub>4</sub> (pH ~ 7) under AM 1.5G illumination. b) Chronoamperometry of system in a) under AM 1.5G illumination in 1.0 M Na<sub>2</sub>SO<sub>4</sub> (pH ~ 7) at 0.61 V vs RHE in a three-electrode setup. The left axis shows photocurrent density while the right axis shows volumetric H<sub>2</sub> production rates during the reaction. c) The left axis shows volumetric O<sub>2</sub> production rates during the chronoamperometry experiment of b). Right axis presents the calculated H<sub>2</sub>: O<sub>2</sub> ratios.

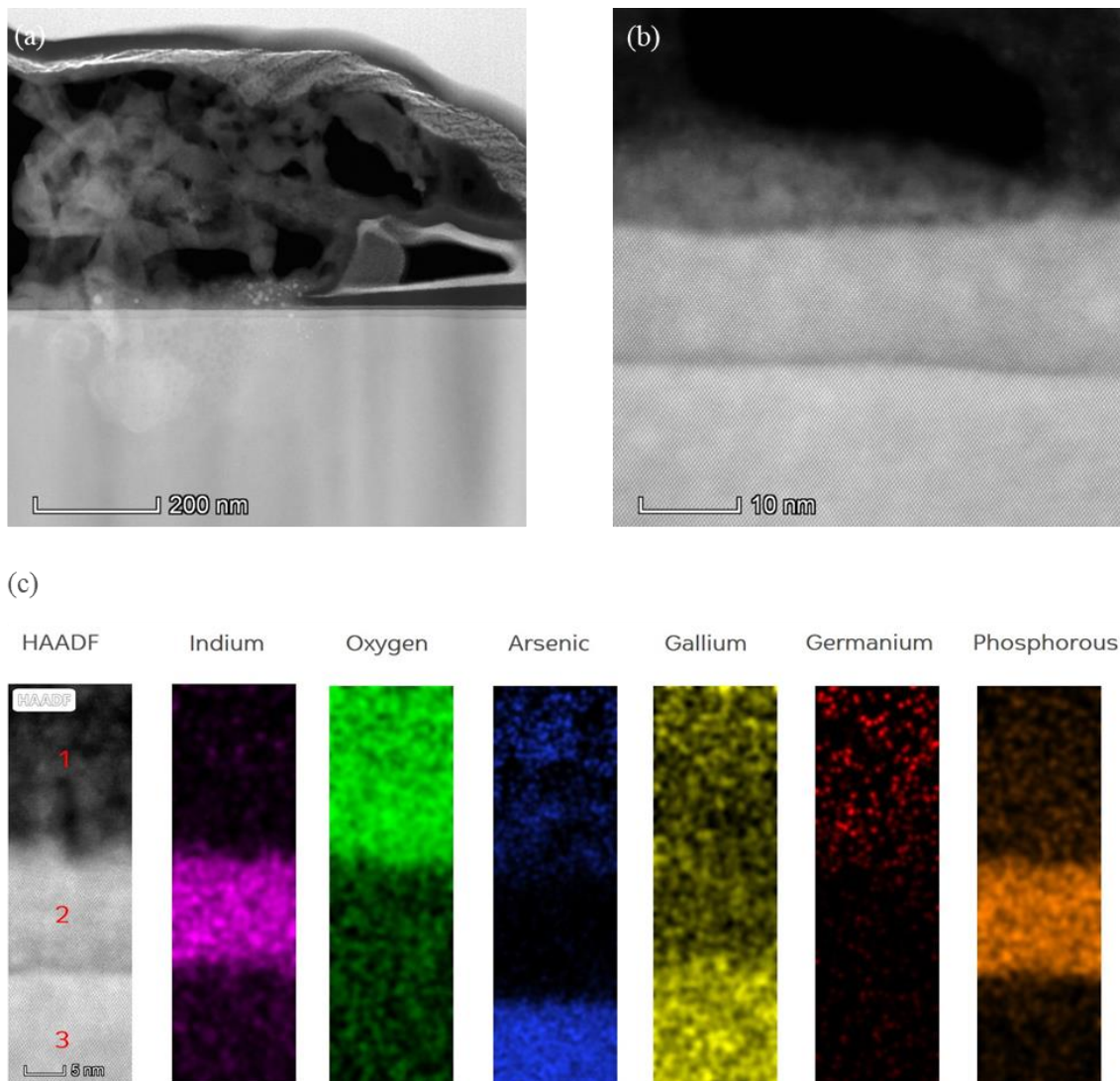


Figure 4. HAADF STEM cross-section images, (a) and (b), of 3J cells after reaction of the experiment presented in Figure 2. (c) Elemental mapping of Indium, oxygen, Arsenic, gallium, germanium, and phosphorous using energy filtering. Note: Scale bar is 5 nm.

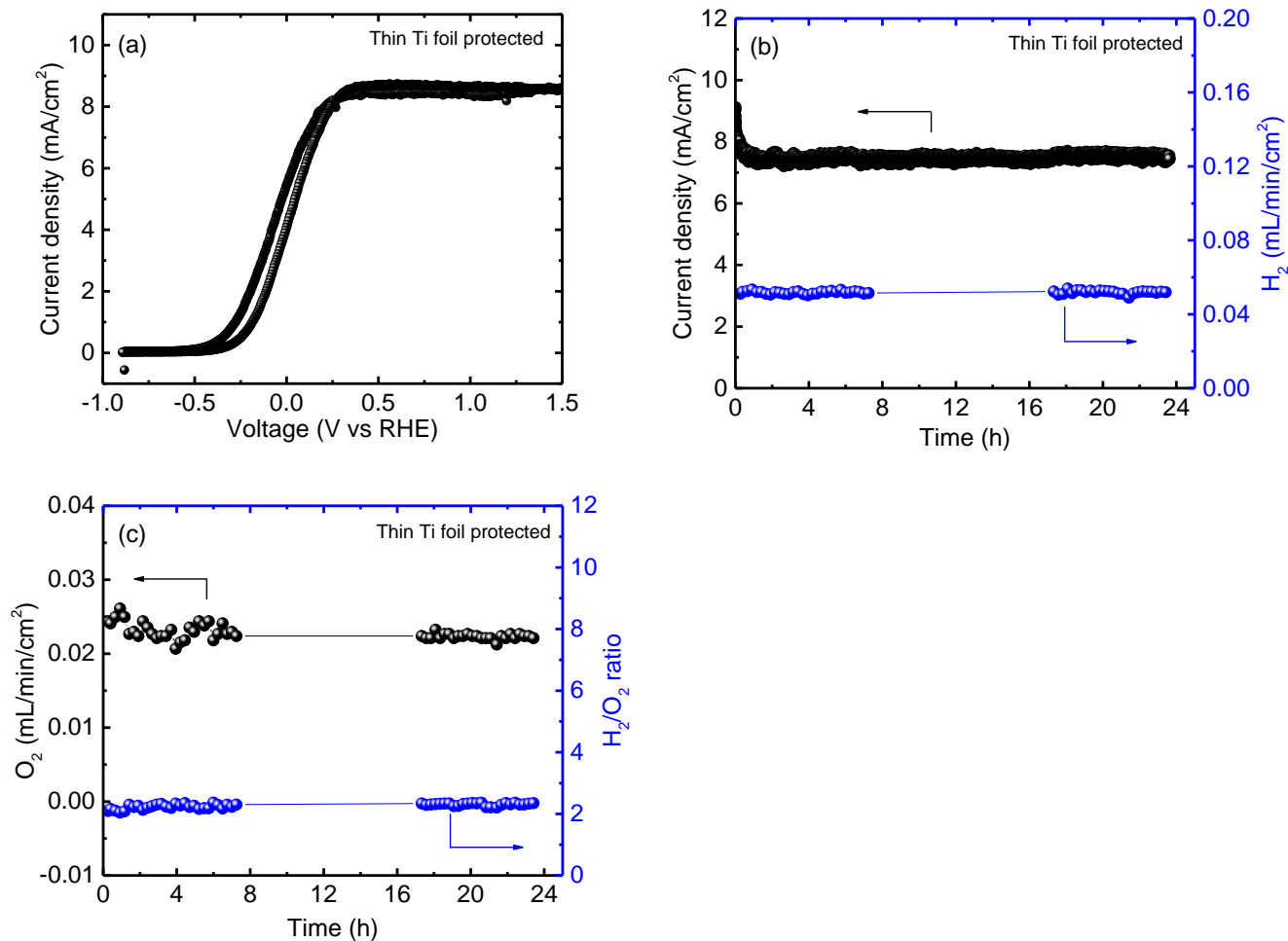
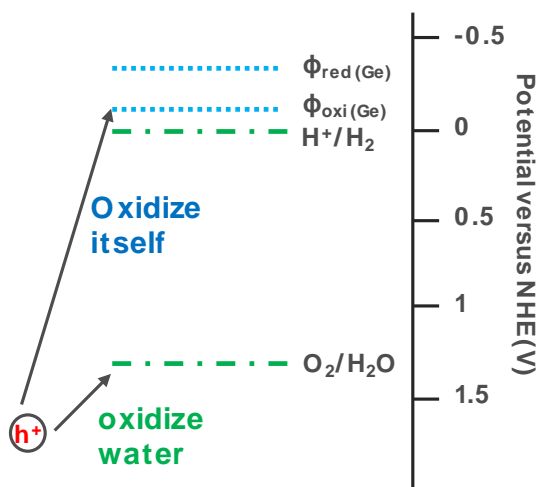


Figure 5. a) Cyclic voltammety (CV) of a thin Ti-foil protected Pt/3J photoanode measured under three-electrode system in 1.0 M Na<sub>2</sub>SO<sub>4</sub> (pH ~ 7) under AM 1.5G illumination. b) Chronoamperometry of the system in a) under AM 1.5G illumination in 1.0 M Na<sub>2</sub>SO<sub>4</sub> (pH ~ 7) at 0.61 V vs RHE in three-electrode setup. The left axis shows photocurrent density while the right axis shows volumetric H<sub>2</sub> production rates during the reaction. c) The left axis shows volumetric O<sub>2</sub> production rates during the chronoamperometry experiment of b). Right axis presents the calculated H<sub>2</sub>: O<sub>2</sub> ratios.

**Scheme 1:**



Energy diagram of the oxidation ( $\phi_{ox}$ ) and reduction potentials ( $\phi_{re}$ ) of Ge versus the oxidation ( $O_2/H_2O$ ) and reduction ( $H^+/H_2$ ) potentials of water. Photogenerated holes ( $h^+$ ) from the 3J cell oxidize the semiconductor rather than water.

**Associated Content:**

**Supporting Information:**

The Supporting Information is available free of charge on the ACS Publications website at DOI: XXXX. Supporting Information contains data for PEC stability testing of the 3J photoanode in a two-electrode setup and TEM images of TiO<sub>2</sub> protected photoanode before and after PEC stability testing.

**Author Information:**

M.A. Khan<sup>1,§</sup>, Purushothaman Varadhan<sup>2,§</sup>, Vinoth Ramalingam,<sup>2</sup> Hicham Idriss<sup>1,\*</sup>, Jr-Hau He<sup>2,3\*</sup>

<sup>1</sup>SABIC-CRD, King Abdullah University of Science and Technology (KAUST), Thuwal, Saudi Arabia.

<sup>2</sup>Computer, Electrical, and Mathematical Sciences and Engineering, KAUST, Thuwal, 23955-6900, Saudi Arabia.

<sup>3</sup>Department of Materials Science and Engineering, City University of Hong Kong, Kowloon, Hong Kong

<sup>§</sup>The authors contributed equally

\*Electronic mail: [jrhauhe@cityu.edu.hk](mailto:jrhauhe@cityu.edu.hk); [idriss@sabir.com](mailto:idriss@sabir.com);

**Acknowledgments:**

The authors acknowledged the financial support from KAUST and Saudi Arabian Basic Industries Corporation (SABIC).

**Notes:**

Views expressed in this Viewpoint are those of the authors and not necessarily the views of the ACS. The authors declare no competing financial interest.

## References:

- Lewis, N. S. Aspects of science and technology in support of legal and policy frameworks associated with a global carbon emissions-control regime. *Energ Environ Sci* **2016**, *9*, 2172-2176.
- Lewis, N. S.; Nocera, D. G. Powering the planet: Chemical challenges in solar energy utilization. *P Natl Acad Sci USA* **2006**, *103*, 15729-15735.
- Szostak, J.; Wilson, D. S.; Hobson, A.; Behrens, T.; Vidal, M.; Brasier, M.; Rayner, S.; Lewis, N.; May, R. 50 ideas to change science Part one Life and Earth. *New Sci* **2010**, *208*, 32-41.
- Su, J. Z.; Vayssieres, L. A Place in the Sun for Artificial Photosynthesis? *Acs Energy Lett* **2016**, *1*, 121-135.
- Lewis, N. S. Toward cost-effective solar energy use. *Science* **2007**, *315*, 798-801.
- Lewis, N. S. Research opportunities to advance solar energy utilization. *Science* **2016**, *351*, 353-+.
- Walter, M. G.; Warren, E. L.; McKone, J. R.; Boettcher, S. W.; Mi, Q.; Santori, E. A.; Lewis, N. S. Solar Water Splitting Cells. *Chem. Rev.* **2010**, *110*, 6446-6473.
- Chen, S. S.; Takata, T.; Domen, K. Particulate photocatalysts for overall water splitting. *Nat Rev Mater* **2017**, *2*, 1-17.
- McKone, J. R.; Lewis, N. S.; Gray, H. B. Will Solar-Driven Water-Splitting Devices See the Light of Day? *Chem Mater* **2014**, *26*, 407-414.
- Walter, M. G.; Warren, E. L.; McKone, J. R.; Boettcher, S. W.; Mi, Q. X.; Santori, E. A.; Lewis, N. S. Solar Water Splitting Cells. *Chem Rev* **2010**, *110*, 6446-6473.
- Fujishima, A.; Honda, K. Electrochemical Photolysis of Water at a Semiconductor Electrode. *Nature* **1972**, *238*, 37-38.
- Hisatomi, T.; Kubota, J.; Domen, K. Recent advances in semiconductors for photocatalytic and photoelectrochemical water splitting. *Chem Soc Rev* **2014**, *43*, 7520-7535.
- Kamat, P. V.; Tvrđy, K.; Baker, D. R.; Radich, J. G. Beyond Photovoltaics: Semiconductor Nanoarchitectures for Liquid-Junction Solar Cells. *Chem Rev* **2010**, *110*, 6664-6688.
- Ager, J. W.; Shaner, M. R.; Walczak, K. A.; Sharp, I. D.; Ardo, S. Experimental demonstrations of spontaneous, solar-driven photoelectrochemical water splitting. *Energ Environ Sci* **2015**, *8*, 2811-2824.
- Sun, K.; Liu, R.; Chen, Y. K.; Verlage, E.; Lewis, N. S.; Xiang, C. X. A Stabilized, Intrinsically Safe, 10% Efficient, Solar-Driven Water-Splitting Cell Incorporating Earth-Abundant Electrocatalysts with Steady-State pH Gradients and Product Separation Enabled by a Bipolar Membrane. *Adv Energy Mater* **2016**, *6*, 1600379, 1-7.
- May, M. M.; Lewerenz, H.-J.; Lackner, D.; Dimroth, F.; Hannappel, T. Efficient direct solar-to-hydrogen conversion by in situ interface transformation of a tandem structure. *Nature Communications* **2015**, *6*, 8286.
- Wen-Hui Cheng, M. H. R., Matthias M May, Jens Ohlmann, David Lackner, Frank Dimroth, Thomas Hannappel, Harry A Atwater, Hans-Joachim Lewerenz. Monolithic Photoelectrochemical Device for Direct Water Splitting with 19% Efficiency. *Acs Energy Lett* **2018**, 1795-1800.
- Brillet, J.; Yum, J.-H.; Cornuz, M.; Hisatomi, T.; Solarska, R.; Augustynski, J.; Graetzel, M.; Sivula, K. Highly efficient water splitting by a dual-absorber tandem cell. *Nature Photonics* **2012**, *6*, 824-828.
- Sun, K.; Liu, R.; Chen, Y.; Verlage, E.; Lewis, N. S.; Xiang, C. A Stabilized, Intrinsically Safe, 10% Efficient, Solar-Driven Water-Splitting Cell Incorporating Earth-Abundant Electrocatalysts with Steady-State pH Gradients and Product Separation Enabled by a Bipolar Membrane. *Advanced Energy Materials* **2016**, *6*, 1600379.
- Verlage, E.; Hu, S.; Liu, R.; Jones, R. J. R.; Sun, K.; Xiang, C.; Lewis, N. S.; Atwater, H. A. A monolithically integrated, intrinsically safe, 10% efficient, solar-driven water-splitting system based on active, stable earth-abundant electrocatalysts in conjunction with tandem III-V light absorbers protected by amorphous TiO<sub>2</sub> films. *Energy & Environmental Science* **2015**, *8*, 3166-3172.
- Paul A. Kempler, M. A. G., Kimberly M. Papadantonakis, and Nathan S. Lewis. Hydrogen Evolution with Minimal Parasitic Light Absorption by Dense Co-P Catalyst Films on Structured p-Si Photocathodes. *Acs Energy Lett* **2018**, 612-617.
- Caban-Acevedo, M.; Stone, M. L.; Schmidt, J. R.; Thomas, J. G.; Ding, Q.; Chang, H. C.; Tsai, M. L.; He, J. H.; Jin, S. Efficient hydrogen evolution catalysis using ternary pyrite-type cobalt phosphosulphide. *Nat Mater* **2015**, *14*, 1245-1251.
- Bae, D.; Seger, B.; Vesborg, P. C. K.; Hansen, O.; Chorkendorff, I. Strategies for stable water splitting via protected photoelectrodes. *Chemical Society Reviews* **2017**, *46*, 1933-1954.
- Hu, S.; Lewis, N. S.; Ager, J. W.; Yang, J.; McKone, J. R.; Strandwitz, N. C. Thin-Film Materials for the Protection of Semiconducting Photoelectrodes in Solar-Fuel Generators. *The Journal of Physical Chemistry C* **2015**, *119*, 24201-24228.



25. Hu, S.; Shaner, M. R.; Beardslee, J. A.; Lichterman, M.; Brunschwig, B. S.; Lewis, N. S. Amorphous TiO<sub>2</sub> coatings stabilize Si, GaAs, and GaP photoanodes for efficient water oxidation. *Science* **2014**, *344*, 1005-1009.
26. Shaner, M. R.; Hu, S.; Sun, K.; Lewis, N. S. Stabilization of Si microwire arrays for solar-driven H<sub>2</sub>O oxidation to O<sub>2</sub>(g) in 1.0 M KOH(aq) using conformal coatings of amorphous TiO<sub>2</sub>. *Energy & Environmental Science* **2015**, *8*, 203-207.
27. Khaselev, O.; Turner, J. A. A monolithic photovoltaic-photoelectrochemical device for hydrogen production via water splitting. *Science* **1998**, *280*, 425-427.
28. Kainthla, R.; Zelenay, B.; Bockris, J. M. Significant efficiency increase in self-driven photoelectrochemical cell for water photoelectrolysis. *Journal of The Electrochemical Society* **1987**, *134*, 841-845.
29. Wang, H.-P.; Sun, K.; Noh, S. Y.; Kargar, A.; Tsai, M.-L.; Huang, M.-Y.; Wang, D.; He, J.-H. High-performance a-Si/c-Si heterojunction photoelectrodes for photoelectrochemical oxygen and hydrogen evolution. *Nano letters* **2015**, *15*, 2817-2824.
30. Yang, F.; Nielander, A. C.; Grimm, R. L.; Lewis, N. S. Photoelectrochemical behavior of n-type GaAs (100) electrodes coated by a single layer of graphene. *The Journal of Physical Chemistry C* **2016**, *120*, 6989-6995.
31. Lee, M. H.; Takei, K.; Zhang, J.; Kapadia, R.; Zheng, M.; Chen, Y. Z.; Nah, J.; Matthews, T. S.; Chueh, Y. L.; Ager, J. W. p-Type InP nanopillar photocathodes for efficient solar-driven hydrogen production. *Angewandte Chemie International Edition* **2012**, *51*, 10760-10764.
32. Dias, P.; Vilanova, A.; Lopes, T.; Andrade, L.; Mendes, A. Extremely stable bare hematite photoanode for solar water splitting. *Nano Energy* **2016**, *23*, 70-79.
33. Liu, R.; Zheng, Z.; Spurgeon, J.; Yang, X. G. Enhanced photoelectrochemical water-splitting performance of semiconductors by surface passivation layers. *Energ Environ Sci* **2014**, *7*, 2504-2517.
34. Verlage, E.; Hu, S.; Liu, R.; Jones, R. J. R.; Sun, K.; Xiang, C. X.; Lewis, N. S.; Atwater, H. A. A monolithically integrated, intrinsically safe, 10% efficient, solar-driven water-splitting system based on active, stable earth-abundant electrocatalysts in conjunction with tandem III-V light absorbers protected by amorphous TiO<sub>2</sub> films. *Energ Environ Sci* **2015**, *8*, 3166-3172.
35. Hu, S.; Shaner, M. R.; Beardslee, J. A.; Lichterman, M.; Brunschwig, B. S.; Lewis, N. S. Amorphous TiO<sub>2</sub> coatings stabilize Si, GaAs, and GaP photoanodes for efficient water oxidation. *Science* **2014**, *344*, 1005-1009.
36. Seger, B.; Pedersen, T.; Laursen, A. B.; Vesborg, P. C. K.; Hansen, O.; Chorkendorff, I. Using TiO<sub>2</sub> as a Conductive Protective Layer for Photocathodic H<sub>2</sub> Evolution. *J Am Chem Soc* **2013**, *135*, 1057-1064.
37. Maeda, K.; Teramura, K.; Takata, T.; Hara, M.; Saito, N.; Toda, K.; Inoue, Y.; Kobayashi, H.; Domen, K. Overall water splitting on (Ga<sub>1-x</sub>Zn<sub>x</sub>)(N<sub>1-x</sub>O<sub>x</sub>) solid solution photocatalyst: Relationship between physical properties and photocatalytic activity. *J Phys Chem B* **2005**, *109*, 20504-20510.
38. Maeda, K.; Takata, T.; Hara, M.; Saito, N.; Inoue, Y.; Kobayashi, H.; Domen, K. GaN : ZnO solid solution as a photocatalyst for visible-light-driven overall water splitting. *J Am Chem Soc* **2005**, *127*, 8286-8287.
39. Kuang, Y. B.; Jia, Q. X.; Ma, G. J.; Hisatomi, T.; Minegishi, T.; Nishiyama, H.; Nakabayashi, M.; Shibata, N.; Yamada, T.; Kudo, A.; Domen, K. Ultrastable low-bias water splitting photoanodes via photocorrosion inhibition and in situ catalyst regeneration. *Nat Energy* **2017**, *2*, 16191, 1-9.
40. Tachibana, Y.; Vayssieres, L.; Durrant, J. R. Artificial photosynthesis for solar water-splitting. *Nature Photonics* **2012**, *6*, 511-518.
41. Wang, Q.; Hisatomi, T.; Jia, Q.; Tokudome, H.; Zhong, M.; Wang, C.; Pan, Z.; Takata, T.; Nakabayashi, M.; Shibata, N.; Li, Y.; Sharp, I. D.; Kudo, A.; Yamada, T.; Domen, K. Scalable water splitting on particulate photocatalyst sheets with a solar-to-hydrogen energy conversion efficiency exceeding 1%. *Nature Materials* **2016**, *15*, 611.
42. Kamat, P. V.; Jin, S. Semiconductor Photocatalysis: "Tell Us the Complete Story!". *ACS Energy Letters* **2018**, *3*, 622-623.
43. Hainer, A. S.; Hodgins, J. S.; Sandre, V.; Vallieres, M.; Lanterna, A. E.; Scaiano, J. C. Photocatalytic Hydrogen Generation Using Metal-Decorated TiO<sub>2</sub>: Sacrificial Donors vs True Water Splitting. *Acs Energy Lett* **2018**, *3*, 542-545.
44. Kenney, M. J.; Gong, M.; Li, Y.; Wu, J. Z.; Feng, J.; Lanza, M.; Dai, H. High-Performance Silicon Photoanodes Passivated with Ultrathin Nickel Films for Water Oxidation. *Science* **2013**, *342*, 836-840.
45. Ponath, P.; Posadas, A. B.; Hatch, R. C.; Demkov, A. A. Preparation of a clean Ge(001) surface using oxygen plasma cleaning. *Journal of Vacuum Science & Technology B* **2013**, *31*, 031201,1-5.
46. Onsia, B.; Conard, T.; De Gendt, S.; Heyns, M.; Hoflijck, I.; Mertens, P.; Meuris, M.; Raskin, G.; Sioncke, S.; Teerlinck, I. A study of the influence of typical wet chemical treatments on the germanium wafer surface. *Solid State Phenomena* **2005**, *103*, 27-30.
47. Yang, J. H.; Cooper, J. K.; Toma, F. M.; Walczak, K. A.; Favaro, M.; Beeman, J. W.; Hess, L. H.; Wang, C.; Zhu, C. H.; Gul, S.; Yano, J. K.; Kisielowski, C.; Schwartzberg, A.; Sharp, I. D. A multifunctional biphasic water splitting catalyst tailored for integration with high-performance semiconductor photoanodes. *Nat Mater* **2017**, *16*, 335-341.

48. Droulers, G.; Beaumont, A.; Beauvais, J.; Drouin, D. Spectroscopic ellipsometry on thin titanium oxide layers grown on titanium by plasma oxidation. *Journal of Vacuum Science & Technology B* **2011**, *29*, 021010.
49. Liu, X.; Chu, P. K.; Ding, C. Surface modification of titanium, titanium alloys, and related materials for biomedical applications. *Materials Science and Engineering: R: Reports* **2004**, *47*, 49-121.